Dynamics of soft and semisoft nematic elastomers

P. I. C. Teixeira* and M. Warner
Cavendish Laboratory, University of Cambridge, Madingley Road, Cambridge CB3 0HE, United Kingdom
(Received 22 January 1999)

We analyze analytically and numerically the dynamics of how a nematic elastomer—an anisotropic rubber—responds elastically and orientationally to an imposed strain. Because positional and orientational degrees of freedom are coupled, the response is not the simple exponential one might expect for a viscous system. Indeed, as a result of this nonlinear coupling, the different modes decay in two qualitatively different ways: with either two distinct or with the same exponential laws, depending, respectively, on whether there is or there is not complete reorientation of the molecular long axes. In addition, at the special values of the strain that form the boundaries between different *equilibrium* behaviors, relaxation is much slower, i.e., it follows a power law. [S1063-651X(99)05107-7]

PACS number(s): 61.30.Cz, 61.41.+e

I. INTRODUCTION

Elastomers are rubbers: networks of weakly cross-linked polymers. The macroscopic shape of an elastomer largely mirrors that of its constituent molecules. Extending a conventional elastomer deforms the network chains away from their natural, most disordered (spherical) shape: the entropy drops and the free energy rises. The free-energy cost of a shape change is what makes an elastomer an elastic solid, even though at the molecular level it has the mobility, fluidity, and disorder of a liquid [1,2].

All this is modified for nematic elastomers, where below a certain temperature chain shapes are not on average spherical, but prolate or oblate spheroidal. First postulated by de Gennes [3,4], these materials were subsequently synthesized by Finkelmann's and Mitchell's groups, as well as by a number of others (see, e.g., [5] and references therein). They are unusual in that they have, coupled to their elasticity deformations, an internal orientational degree of freedom, namely their nematic order: the molecular long axes align preferentially along one particular direction, termed the nematic director. Now, a distorted distribution of chain shapes is not the only possible response to an extension or a shear: this distribution can be rotated without distortion, hence at constant entropy, in such a way that the macroscopic sample shape is still mirrored by that of the constituent molecules (see Fig. 1). This being the case, the free energy does not rise and the shape change is achieved as if the elastomer were a liquid. One requires that the nematic director rotate as the deformation proceeds. This shape-nematic coupling is what generates the remarkable soft elasticity, first predicted on phenomenological grounds by Golubovic and Lubensky [6] within continuum theory.

The elasticity of these solid liquid crystals has been much studied experimentally and theoretically. Besides macroscopic sample changes on ordering nematically [7,8], they exhibit exotic properties such as memory effects [9], stress-induced molecular switching [10], strain-induced discontinuous director rotation (predicted by Bladon, Terentjev, and Warner [11] and seen by Mitchell and co-workers [12]), the so-called ''stripe domains'' [13], and the analog of a Freederiks transition [14]. The last two effects have been interpreted [15–17] in terms of the ''neoclassical'' molecular theory of nematic elastomers [18], which is able to handle nonlinearities and discontinuities.

Here we wish to examine the dynamics of relaxation of a nematic elastomer which has been stretched at right angles to the director. This will be complicated, since on distortion both positional and orientational modes respond. The softest trajectory involves the coupled viscoelastic motion of shear and director modes. If the material is truly soft, i.e., if it supports deformations that cost no free energy, there should be a vanishing driving force for this motion and the response will be slow. Both ideal and real nematic elastomers have conventional and soft (or semisoft) regimes, depending on the magnitude of the imposed extensional strain. We have found that the dynamics should be qualitatively different in the two elastically qualitatively different regimes. In one case the coupled modes should relax with different rates depending on the underlying positional and orientational mobilities. Remarkably, in the other case the modes should mix and relax with a single rate. This unusual result is shown to be a consequence of the anomalous elastic behavior possible in nematic elastomers. A closely related system has yielded experimental data: Meyer *et al.* [14] instead rotate the director by applying an electric field, and on removing the field

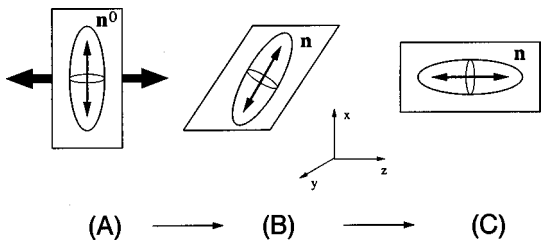

FIG. 1. Experimental geometry considered: At $t=0$, the nematic director $\mathbf{n}^0$ is along the x axis. Application of a strain along z rotates the chain shape distribution so that as $t\to\infty$ the director points along z (regime C) or some intermediate angle (regime B). In addition to extension, the shear $\delta=\lambda_{zx}$ is allowed.

*Present address: IRC in Polymer Science and Technology, Department of Physics, University of Leeds, Leeds LS2 9JT, U.K.

there is an overdamped viscous relaxation of the director. A subsequent study [17] has revealed that this distortion involves other coupled mechanical modes. By contrast, the anisotropic gels of Hikmet and Boots [19] also respond to applied electric fields but, unlike Meyer *et al.*'s [14] or Clarke and Terentjev's [20] elastomers, they appear to be microphase-separated structures, since they scatter light in their field-on state and have much shorter (by a factor of 1000) switching times, typical of free (un-cross-linked) liquid crystals.

This paper is organized as follows. In Sec. II we briefly review the neoclassical theory of (Gaussian) elastomer elasticity [1,2] and write down the corresponding free-energy density of a nematic elastomer. We then derive the equations of motion that are solved analytically, in the long-time limit, in Sec. III, and numerically, over the whole time range, in Sec. IV. Finally, in Sec. V we summarize our conclusions. Details of the asymptotic analysis of the equations of motion are given in the Appendix.

II. THE FREE ENERGY AND EQUATIONS OF MOTION

The first, linear, continuum picture of nematic elastomers is due to de Gennes [21], who wrote down the (phenomenological) free-energy density:

$$f_{\rm rot}=\frac{1}{2}D_1[(\Omega-\omega)\times\mathbf{n}]^2+D_2\mathbf{n}\cdot\underline{\underline{e}}\cdot[(\Omega-\omega)\times\mathbf{n}], \quad (1)$$

where Ω and ω are the rotations of the elastic matrix and of the director $\mathbf{n}$, respectively, with respect to some fixed axis, and $\underline{\underline{e}}$ is the infinitesimal deformation tensor. The two energy scales D_1 and D_2 penalize, respectively, director rotations with respect to the polymer matrix, and shear deformations of the polymer matrix relative to the director. Still, because elastomers are essentially liquidlike, they are capable of huge extensions, and it is in the nonlinear limit that the most interesting phenomena are observed. One then requires the nematic equivalent of the molecular theory of rubber elasticity to derive the free energy up to distortions of several hundred percent.

A. The free energy

The neoclassical theory of ordinary rubber elasticity treats a polymer chain as a Gaussian random walk [1,2]; the distribution of end-to-end distances $\mathbf{R}$ is thus

$$P_{\rm isot}(\mathbf{R})\sim\exp\left(-\frac{3\mathbf{R}^2}{2l\mathcal{L}}\right), \quad (2)$$

with l the step length and $\mathcal{L}$ the arc length between cross links, assumed sufficiently long (or the corresponding number of monomer units large). The free energy of two connected cross links $\mathbf{R}$ apart is

$$F_{\rm isot}(\mathbf{R})=-k_BT\ln P_{\rm isot}(\mathbf{R})=k_BT\frac{3\mathbf{R}^2}{2l\mathcal{L}}, \quad (3)$$

where k_B is Boltzmann's constant and T is the temperature. $F_{\rm isot}(\mathbf{R})$ is of purely entropy origin: the closer two points are, the more configurations are available to the chain connecting them, and therefore the lower the free energy. This is also true if sufficiently long, nematic chains are *anisotropic* random walks; we then have, instead of Eq. (2),

$$P_{\rm nem}(\mathbf{R})\sim\exp\left(-\frac{3}{2l\mathcal{L}}\mathbf{R}^T\underline{\underline{\ell}}^{-1}\mathbf{R}\right). \quad (4)$$

The chain shape distribution is Gaussian, characterized by an *anisotropic* (second-moment) shape spheroid $\underline{\underline{\ell}}^0$ before and $\underline{\underline{\ell}}$ after deformation. $\underline{\underline{\ell}}$ is essentially the tensor of step lengths describing the polymer random walk statistics. It is uniaxial, aligned with the director $\mathbf{n}$:

$$\underline{\underline{\ell}}=\ell_\perp\underline{\underline{I}}+(\ell_\parallel-\ell_\perp)\mathbf{nn}, \quad (5)$$

where $\underline{\underline{I}}$ is the unit tensor, $\mathbf{nn}$ is a dyad, and $\ell_\perp$ and $\ell_\parallel$ are the step lengths perpendicular and parallel to $\mathbf{n}$, respectively. Typically, if we measure $\underline{\underline{\lambda}}$ directly from the relaxed state before deformation (and not from some state more distant in the thermomechanical history), then $\underline{\underline{\ell}}$ and $\underline{\underline{\ell}}^0$ differ only in the directions $\mathbf{n}$ and $\mathbf{n}^0$, and not in the magnitude of their elements. The free-energy density (FED) for nematic elastomers then follows from a quenched average of $\ln P_{\rm nem}(\mathbf{R})$ with the statistical weight at network formation $P^0_{\rm nem}(\mathbf{R}^0)$ [18]:

$$f=\frac{1}{2}n_sk_BT\,\mathrm{Tr}[\underline{\underline{\ell}}^0\cdot\underline{\underline{\lambda}}^T\cdot\underline{\underline{\ell}}^{-1}\cdot\underline{\underline{\lambda}}], \quad (6)$$

where n_s is the number of elastically active polymer strands per unit volume in the network and Tr denotes the trace of a matrix. The deformation $\underline{\underline{\lambda}}$ transforms an initial point $\mathbf{R}^0$ into a final point $\mathbf{R}$, that is, $\mathbf{R}=\underline{\underline{\lambda}}\mathbf{R}^0$.

Extracting factors of $\ell_\perp$ from $\underline{\underline{\ell}}^0$ and from $\underline{\underline{\ell}}$, which then cancel in Eq. (6), we can characterize $\underline{\underline{\ell}}$ and $\underline{\underline{\ell}}^0$ instead by $r=\ell_\parallel/\ell_\perp$. Then $\underline{\underline{\ell}}$ can be rewritten as

$$\underline{\underline{\ell}}=\underline{\underline{I}}+(r-1)\mathbf{nn}. \quad (7)$$

r is a measure of the chain anisotropy and can be large. One can show [18] that the spontaneous extension along the director, λ_m, of an unconstrained sample on entering the nematic phase from the isotropic phase, is $\lambda_m=r^{1/3}$. This can be as much as 50% (i.e., $\lambda_m=1.5$), yielding $r\sim3.4$. Note that isotropic chains have $r=1$, whereupon Eq. (6) reduces to the classical expression for rubber elasticity.

As mentioned in the Introduction, there exists a continuum of soft deformations that leave the FED unchanged at its relaxed value, $f=\frac{3}{2}n_sk_BT$. These are of the general form $\underline{\underline{\lambda}}=\underline{\underline{\ell}}^{1/2}\cdot\underline{\underline{U}}\cdot(\underline{\underline{\ell}}^0)^{-1/2}$, where $\underline{\underline{U}}$ is an arbitrary rotation matrix [22]. In this paper we shall restrict ourselves to strains given by

$$\underline{\underline{\lambda}}=\begin{pmatrix}\lambda_{xx}&0&0\\0&\lambda_{yy}&0\\\delta&0&\lambda\end{pmatrix}, \quad (8)$$

where (see Fig. 1) the sample is extended by a factor λ in the direction perpendicular to the original director $\mathbf{n}^0$ $(\equiv\hat{\mathbf{x}})$, allowing transverse relaxations λ_{xx} and $\lambda_{yy}=1/(\lambda_{xx}\lambda)$ (since

deformations are at constant volume in such soft materials). In addition, we allow a shear relaxation $\delta=\lambda_{zx}$, which helps accommodate the rotating molecular spheroids and ensures that such deformations are soft up to a threshold $\lambda=\lambda_2$, where director rotation is complete. The softness of response and the director rotation on extension have been studied by Kundler and Finkelmann [13] and by Talroze *et al.* [23]. They also see stripes and more complex patterns, presumably because of the difficulties in accommodating δ at the clamps where the sample is gripped. We ignore the larger-scale problems of stripes and inhomogeneities in the clamp region and concentrate instead on uniform deformations $\underline{\underline{\lambda}}$ and uniform director rotations θ (the latter defined as the angle between the director and the x axis). Inserting Eq. (7) for $\underline{\underline{\ell}}$ and Eq. (8) for $\underline{\underline{\lambda}}$ into Eq. (6), we obtain the FED

$$f=\frac{1}{2}n_s k_B T\Bigg[\lambda^2+\lambda_{xx}^2+\frac{1}{(\lambda_{xx}\lambda)^2}+r\delta^2-(r-1)\lambda_{xx}\delta\sin 2\theta -(r-1)\left(\frac{\lambda^2}{r}-\lambda_{xx}^2+\delta^2\right)\sin^2\theta\Bigg], \tag{9}$$

to which must be added a term $f_{ss}=\frac{1}{2}n_s k_B T A\lambda^2\sin^2\theta$, the so-called ''semisoft'' deviation from completely soft elasticity. Such nonideality stems from the elastomer's thermomechanical history, for instance the order parameter imposed during cross-linking to achieve a macroscopic monodomain. It gives a small threshold $\lambda_1=[(1-1/r)/(1-1/r-A)]^{1/3}>1$ above which the material responds with a low stress until the director rotation is complete at $\lambda_2=\sqrt{r}\lambda_1$; there are thus three regimes of response. Straightforwardly, minimizing the semisoft FED, $f+f_{ss}$, over δ, λ_{xx} and θ yields (see [15] for details)

$$\mathsf{A}:\ \lambda<\lambda_1,\quad \bar{\theta}=0,\quad \bar{\lambda}_{xx}=\bar{\lambda}_{yy}=\frac{1}{\sqrt{\lambda}},\quad \bar{\delta}=0; \tag{10}$$

$$\mathsf{B}:\ \lambda_1<\lambda<\lambda_2,\quad \sin^2\bar{\theta}=\frac{r}{r-1}\left(1-\frac{\lambda_1^2}{\lambda^2}\right),$$

$$\bar{\lambda}_{xx}=\frac{\sqrt{\lambda_1}}{\lambda},\quad \bar{\lambda}_{yy}=\frac{1}{\sqrt{\lambda_1}},$$

$$\bar{\delta}=\frac{r-1}{2r}\frac{\lambda}{\lambda_1^{3/2}}\sin 2\bar{\theta}; \tag{11}$$

$$\mathsf{C}:\ \lambda>\lambda_2,\quad \bar{\theta}=\frac{\pi}{2},\quad \bar{\lambda}_{xx}=\frac{1}{r^{1/4}\sqrt{\lambda}},\quad \bar{\lambda}_{yy}=\frac{r^{1/4}}{\sqrt{\lambda}},\quad \bar{\delta}=0, \tag{12}$$

where an overbar over a variable denotes its equilibrium value. Regime A corresponds to no rotation of the director; regime B, to partial rotation towards the direction of extension; and regime C, to complete reorientation. The behavior is qualitatively the same for $A=0$ $(\lambda_1=1)$ and $A>0$ $(\lambda_1>1)$; for instance, the singular dependence of $\theta(\lambda)$ as seen by Kundler and Finkelmann [13] and collapsed to Eq. (11) for a large number of elastomers by Finkelmann *et al.* [16]. Equally, normal (isotropic) elastomers have a $1/\sqrt{\lambda}$ transverse relaxation, seen here in regimes A and C. By contrast, in the soft or semisoft regime B we have $1/\lambda$ and constant contraction/dilation in the x and y directions, respectively. Regime A has been studied by one of us [24], in the special case where only shears are allowed (i.e., $\lambda=\lambda_{xx}=1$) and the director returns to $\bar{\theta}=0$ on switching off a disaligning electric field.

B. The equations of motion

The relaxation of this system, governed as it is by nonconserved variables, is most simply modeled in a continuum fashion with mobilities Γ_α $(\alpha=\theta,\lambda_{xx},\delta)$ giving the rate of response of each variable to the corresponding generalized force deriving from the FED:

$$\frac{d\theta}{dt}=-\Gamma_\theta\frac{\partial f}{\partial\theta} =-\Gamma_\theta\Bigg[A\lambda^2\sin 2\theta-2\delta\lambda_{xx}(r-1)\cos 2\theta -\left(\delta^2-\lambda_{xx}^2+\frac{\lambda^2}{r}\right)(r-1)\sin 2\theta\Bigg], \tag{13}$$

$$\frac{d\lambda_{xx}}{dt}=-\Gamma_\lambda\frac{\partial f}{\partial\lambda_{xx}} =-\Gamma_\lambda\Bigg[2\lambda_{xx}-\frac{2}{\lambda^2\lambda_{xx}^3}+2\lambda_{xx}(r-1)\sin^2\theta -\delta(r-1)\sin 2\theta\Bigg], \tag{14}$$

$$\frac{d\delta}{dt}=-\Gamma_\delta\frac{\partial f}{\partial\delta} =-\Gamma_\delta[2\delta r-2\delta(r-1)\sin^2\theta-\lambda_{xx}(r-1)\sin 2\theta], \tag{15}$$

where we have absorbed a factor of $\frac{1}{2}n_s k_B T$ into the definitions of Γ_α, and for simplicity have written $\Gamma_{\lambda_{xx}}$ as Γ_λ. An analogous problem has been addressed by us, namely where extensions and contractions are suppressed $(\lambda=\lambda_{xx}=\lambda_{yy}=1)$ but shears δ and director rotation are allowed under an electric field applied perpendicular to the initial direction of alignment [17,24]. Its statics and dynamics have been investigated experimentally by Meyer *et al.* [14].

The evolution Eqs. (13)–(15) describe the approach to the equilibrium state, given by equations (10)–(12), upon imposition of an extension λ. We shall look in detail into regimes B and C. There is no internal rotation of the elastomer under an extension λ in regime A except for the transverse, volume-preserving relaxations to $1/\sqrt{\lambda}$. These must occur at a rate governed by the speed of longitudinal sound. In regimes B and C we shall consider the initial state of the system to be not only λ $(>\lambda_1)$ but also $\lambda_{xx}=\lambda_{yy}=1/\sqrt{\lambda}$, the latter two variables attaining this (nonequilibrium) state in a time derived from propagating elastic waves across the sample, a time that is much shorter than the smallest Γ_α^{-1},

which derives from the subsequent internal relaxation. Equations (13)–(15) are coupled, so that the evolution of each variable is driven by the deviations of all variables from equilibrium. This can be understood in the context of our earlier discussion of why a shear δ is necessary to accommodate shape change due to director rotation. Furthermore, it opens up the possibility of complex behavior, depending on the ratios of the dynamical rates Γ_α.

In the next section we linearize the above equations of motion for $\lambda(t)$ and $\theta(t)$, in order to extract their asymptotic behavior at long times and thereby clarify the qualitative aspects of the approach to equilibrium. It turns out that λ_{xx} becomes decoupled from the other two variables at linear order in regime C, leading to unexpected results. These are then confirmed by numerical solutions, presented in Sec. IV. We shall presume similar relaxation mechanisms for the positional modes δ and λ_{xx}, and accordingly set $\Gamma_\delta = \Gamma_\lambda$ in what follows. Cases will be considered where the nematic degree of freedom, $\theta(t)$, is comparably fast, faster, or slower than the positional degrees of freedom.

We shall see that the coupled, dissipative equations of motion generally yield exponential decays of the observables. Yet it is known that the long-time response of both isotropic [25] and nematic [26] elastomers is very slow indeed. These are very subtle effects of chain connectivity, stress localization, and, in nematic elastomers, random fields causing competing orderings. Polydomain elastomers have, additionally, pinning, activation, and competition and compatibility issues. Work by Clarke and Terentjev [26], both experimental and theoretical, shows that their response to imposed strains is highly nontrivial and with a very slow dynamics. Our investigation is then clearly only applicable to times early compared with the very long time scales associated with these other processes. Setting aside this long-time relaxation, there is nevertheless experimentally rich behavior observed in the earlier, principal decay of strains. We have mentioned the dynamics induced by electric field coupling to the director [14]. There are also the dynamical mechanical measurements of Clarke and Terentjev [20], which reveal relaxation in the fraction-of-second regime, a motion apparently of the type we examine here.

III. THE APPROACH TO EQUILIBRIUM: ASYMPTOTIC ANALYSIS

In the long-time limit, as deviations from the final equilibrium values become small, Eqs. (13)–(15) can be linearized to give

$$\frac{d}{dt}\begin{pmatrix} \Delta\theta \\ \Delta\lambda_{xx} \\ \Delta\delta \end{pmatrix} = -\underline{\underline{M}}\cdot\begin{pmatrix} \Delta\theta \\ \Delta\lambda_{xx} \\ \Delta\delta \end{pmatrix}, \tag{16}$$

where $\Delta\theta = \theta - \bar{\theta}$, $\Delta\lambda_{xx} = \lambda_{xx} - \bar{\lambda}_{xx}$, $\Delta\delta = \delta - \bar{\delta}$ are the deviations of the relaxing variables away from their final equilibrium values. $\underline{\underline{M}}$ is given in terms of $\bar{\theta}$, $\bar{\lambda}_{xx}$, $\bar{\delta}$; it differs qualitatively in form depending on whether λ is in regime B or C. Explicit expressions for the elements of $\underline{\underline{M}}$ are presented in the Appendix. One sees that for $r=1$ (isotropic elastomer), the dynamics in the variable θ disappears and λ_{xx} and δ decouple from each other, as expected in a conventional solid.

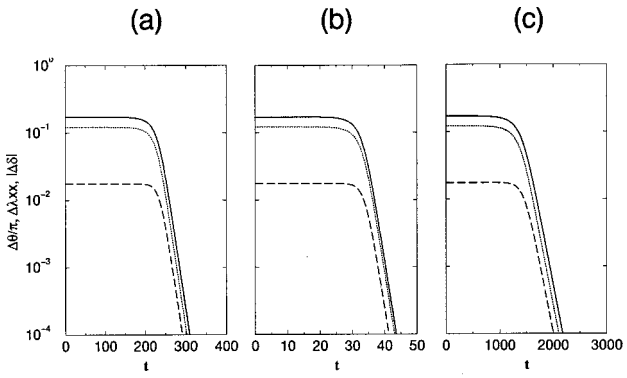

FIG. 2. $\Delta\theta$ (solid line), $\Delta\lambda_{xx}$ (dashed line), and $|\Delta\delta|$ (dotted line) for a nematic elastomer characterized by $r=1.4$, $A=0.1$, and (a) $\Gamma_\theta/\Gamma_\lambda = 1.0$; (b) $\Gamma_\theta/\Gamma_\lambda = 10.0$; and (c) $\Gamma_\theta/\Gamma_\lambda = 0.1$. The extension is $\lambda = 1.2$ (regime B). At long times, all three variables decay exponentially with the same time constant (see the text and Table I for details).

A. Regime B

The rate matrix $\underline{\underline{M}}$ is 3×3 and has three real eigenvalues, μ_1, μ_2, μ_3, with corresponding eigenvectors $\mathbf{v}_1, \mathbf{v}_2, \mathbf{v}_3$, decaying as pure exponentials: $\mathbf{v}_i(t) = \mathbf{v}_i(0)e^{-\mu_i t}$ $(i=1,2,3)$. $\Delta\theta(t)$, $\Delta\lambda_{xx}(t)$, and $\Delta\delta(t)$ can be expressed as linear combinations of the $\mathbf{v}_i(t)$ and hence will be the sum of exponential decays. At long times, whatever the admixture of $\mathbf{v}_1, \mathbf{v}_2, \mathbf{v}_3$ in a given variable is, the behavior will be dominated by the slowest mode, that is, the mode with the smallest μ_i, μ_s, say. And indeed the variables in Figs. 2 and 3 all relax with the *same* rate constant in the long-time region. The smallest of the calculated eigenvalues of $\underline{\underline{M}}$ for the two λ's in regime B agrees exactly with the rate obtained by fitting the numerical curves (see Tables I and II). The preasymptotic knee seen in Figs. 2 and 3 is a consequence of the presence of faster-decaying modes. In the Appendix we demonstrate that the matrix of decay rates $\underline{\underline{M}}$ becomes singular at the beginning and end of regime B, that is, at $\lambda = \lambda_1$ and $\lambda = \lambda_2$. At these particular elongations parts of the problem become purely nonlinear and the dynamics power law rather than exponential.

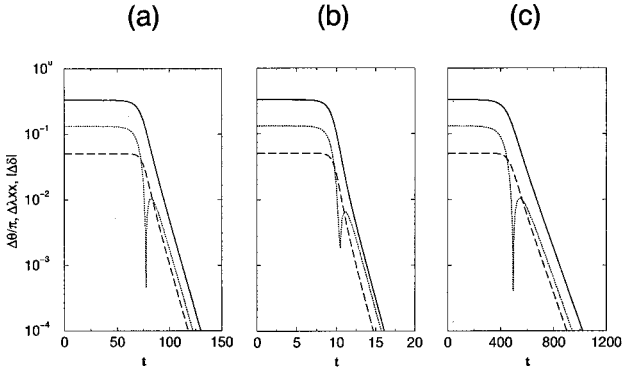

FIG. 3. Same as Fig. 2 but for $\lambda = 1.3$ (regime B). See the text and Table II for details.

TABLE I. Elastomer relaxation to regime B, $\lambda=1.2$, for $r=1.4$, $A=0.1$, $\Gamma_\lambda=\Gamma_\delta=1.0$. μ_s is the smallest eigenvalue of $\underline{\underline{M}}$ given by Eqs. (A1)–(A9) of the Appendix. The decay rates are found by fitting the curve for $\Delta\theta(t)$ in Fig. 2 to an exponential. The numbers in parentheses are the estimated uncertainties in the last decimal places; note the excellent agreement between analytical predictions and numerical results.

Γ_θ	μ_s	Decay rate
1.0	0.092 8004	0.092 64(1)
10.0	0.695 105	0.691 2(6)
0.1	0.009 524 23	0.009 5131(5)

B. Regime C

When the final state is of total reorientation, $\overline{\theta}=\pi/2$, and zero shear, $\overline{\delta}=0$, the linearization of the equations of motion is more subtle since several elements of **M** vanish; see the Appendix. The equation for $\Delta\lambda_{xx}$ decouples from those for $\Delta\theta$ and $\Delta\delta$, which remain coupled to each other. One can immediately see why at long times $\Delta\theta$ and $\Delta\delta$ must have the same decay rate—it will be the smaller of the two eigenvalues emerging when the 2×2 problem of $(\Delta\theta,\Delta\delta)$ (described by matrix $\underline{\underline{M}}_{\rm red}$, see the appendix) is broken down into normal modes.

The equation for $\Delta\lambda_{xx}$, being decoupled, has a dynamics of its own and is, superficially,

$$\frac{d\Delta\lambda_{xx}}{dt}=-8\Gamma_\lambda r\Delta\lambda_{xx}. \tag{17}$$

However, there is no *a priori* reason for discarding the higher-order terms in $(\Delta\theta)^2$, $\Delta\theta\Delta\delta$, and $(\Delta\delta)^2$ in Eq. (17), which are, at linear order, independent of $\Delta\lambda_{xx}$. Although of second order, they may or may not be smaller than the other driving term, $\Delta\lambda_{xx}$. Retaining them, one obtains instead

$$\frac{d\Delta\lambda_{xx}}{dt}=-8\Gamma_\lambda r\Delta\lambda_{xx}+2\Gamma_\lambda(r-1)\left[\frac{1}{r^{1/4}\sqrt{\lambda}}(\Delta\theta)^2-\Delta\theta\Delta\delta\right]$$
$$=-8\Gamma_\lambda r\Delta\lambda_{xx}+g(t), \tag{18}$$

where $g(t)$ is a known function, as $\Delta\theta(t),\Delta\delta(t)$ are determined separately as solutions of the decoupled 2×2 problem. At long times both must decay exponentially with the lowest eigenvalue μ_s of $\underline{\underline{M}}_{\rm red}$, determining the rate as discussed above. Thus $g(t)\tilde{=}\mathcal{B}\exp(-2\mu_s t)$ and Eq. (18) is a simple nonhomogeneous ordinary differential equation with solution

$$\Delta\lambda_{xx}(t)=\mathcal{B}_c e^{-8\Gamma_\lambda r t}+\mathcal{B}\frac{e^{-2\mu_s t}}{8\Gamma_\lambda r-2\mu_s}, \tag{19}$$

TABLE II. Same as Table I, but for $\lambda=1.3$, using Fig. 3.

Γ_θ	μ_s	Decay rate
1.0	0.128 968	0.129 06(1)
10.0	1.018 54	1.019 4(1)
0.1	0.013 1045	0.013 1085(3)

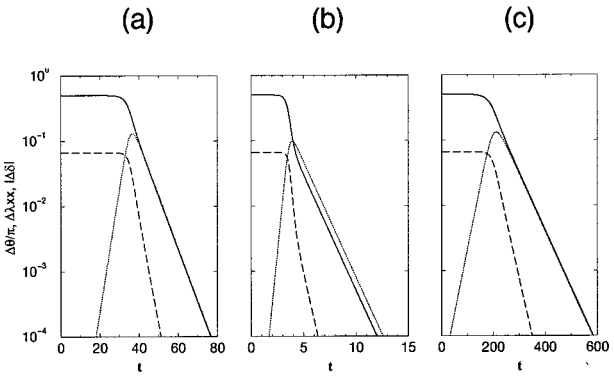

FIG. 4. $\Delta\theta$ (solid line), $\Delta\lambda_{xx}$ (dashed line), and $|\Delta\delta|$ (dotted line) for a nematic elastomer characterized by $r=1.4$, $A=0.1$, and (a) $\Gamma_\theta/\Gamma_\lambda=1.0$; (b) $\Gamma_\theta/\Gamma_\lambda=10.0$; and (c) $\Gamma_\theta/\Gamma_\lambda=0.1$. The extension is $\lambda=1.5$ (regime C). δ starts from zero and only when it is appreciable are the other variables seen to react, as there must exist enough shear to accommodate $\Delta\theta$, see Fig. 1. At long times, all three variables decay exponentially but the rate constant of $\Delta\lambda_{xx}$ is twice those of the other two, which are equal (see the text and Table III for details).

where $\mathcal{B}_c$ is an arbitrary constant. Now it is clear from Eq. (A11) of the Appendix that $\mu_s\ll4\Gamma_\lambda r$, for most choices of Γ_θ and Γ_δ. This means that $\Delta\lambda_{xx}(t)$ is dominated by the nonhomogeneous term, that is, by the effect of $\Delta\theta(t)$ and $\Delta\delta(t)$. It follows that the rate of decay of $\Delta\lambda_{xx}(t)$ is twice that of $\Delta\theta(t)$ or $\Delta\delta(t)$:

$$\Delta\lambda_{xx}(t)\sim e^{-2\mu_s t}\sim(\Delta\theta(t))^2\sim(\Delta\delta(t))^2. \tag{20}$$

Because the dynamics is singular at $\lambda=\lambda_1$ and $\lambda=\lambda_2$, there are always regions of λ where some eigenvalues become very small and the time scales in Eq. (19) are well separated, hence where Eq. (20) is valid.

The remarkable qualitative change between regimes B and C is borne out by the numerical results of Sec. IV. Once more, the faster-decaying mode manifests itself as the knee in Fig. 4.

IV. NUMERICAL SOLUTIONS

We adopt a typical value of the anisotropy $r=1.4$ [23] and a moderate semisoftness $A=0.1$ [17]. For these choices the threshold for deformations is $\lambda_1\approx1.154$, and that for completion of the (semi)soft regime is $\lambda_2\approx1.366$. In this section, time is given in units of $\Gamma_\lambda=\Gamma_\delta$. NAG library routine D02BDF was used to perform the numerical integration (Runge-Kutta-Merson method).

A. Relaxation to regime B

In Fig. 2 we show the relaxation in response to an imposed deformation $\lambda=1.2$. Since the system starts in a metastable state [setting $\theta=\delta=0$ in Eqs. (13)–(15) will confirm that there is initially no motion], a small misalignment of θ ($10^{-6}-10^{-4}$ is enough) is required to start off. To this extent the origin in time is arbitrary and we do not display the initial decay.

Irrespective of the relative dynamical rates, $\Gamma_\theta:\Gamma_\lambda:\Gamma_\delta$, the early time behavior is identical, with $\Delta\theta$ and $\Delta\delta$ starting

TABLE III. Elastomer relaxation to regime C, $\lambda=1.5$, for $r=1.4$, $A=0.1$, $\Gamma_\lambda=\Gamma_\delta=1.0$. μ_s is the smallest eigenvalue of $\underline{\underline{M}}_{\rm red}$ given by Eq. (A10) in the Appendix. The decay rates are found by fitting the curve for $\Delta\theta(t)$ in Fig. 4 to an exponential. The numbers in parentheses are the estimated uncertainties in the last decimal places. Once more, the agreement between analytical predictions and numerical results is remarkable.

Γ_θ	μ_s	Decay rate
1.0	0.186 161	0.186 166(1)
10.0	0.812 649	0.812 666(4)
0.1	0.020 2819	0.020 301 5(7)

first and more gradually than $\Delta\lambda_{xx}$. At longer times the decays are very accurately single exponential (see Table I), with exactly the same time scale for all three variables, as follows from the analysis of the preceding section. The same observations can be made of Fig. 3, where $\lambda=1.3$ (see also Table II). A little more structure is nonetheless evident in $\delta(t)$, even though the system is overdamped: the shear does not approach its equilibrium value monotonically, and thus $\Delta\delta$ changes sign at some intermediate time. (The cusp in Fig. 3 is a consequence of plotting $|\Delta\delta|$.) This results from the fact that the components of the combination of distortions coupled to, and hence driving, $\delta(t)$, themselves decay at different rates. Moreover, it is apparent particularly in the $\Gamma_\theta=10$ case that there is a knee in going from the initial regime to the late-time region with its common slope.

B. Relaxation to regime C

A strain of $\lambda=1.5$ is now imposed. The response of the various modes is outwardly rather complex (see Fig. 4): $\Delta\delta$ starts at zero, since in regime C both the initial and final shear vanish. The shear seems to take off more rapidly than $\Delta\theta$ or $\Delta\lambda_{xx}$ but this is illusory as it starts from zero and small changes are simply more visible. There is again a knee in $\Delta\theta$ and $\Delta\lambda_{xx}$. The final decay is purely exponential with the rate of $\Delta\lambda_{xx}$ exactly twice those of $\Delta\theta$ and $\Delta\delta$, which are equal (see Table III). These remarks hold for all ratios $\Gamma_\theta:\Gamma_\lambda:\Gamma_\delta$. Thus as revealed analytically in Sec. III, there is both complexity and universality in the response.

V. CONCLUSIONS

We have examined the response of a highly unusual elastic material to step extensions. The coupling between mechanical and internal (orientational) modes gives rise to different dynamics depending on whether the nematic elastomer is extended to be in the (semi)soft regime or in the hard region beyond, in which director reorientation is complete. The most striking prediction is that in the latter regime the rate of transverse mechanical relaxation should be twice the rate of director reorientation.

We should stress that our analysis is for the not-too-late stages of the behavior of nematic monodomains, so that the subtle long-time effects found even in isotropic elastomers do not prevail. However, the dynamics of reorientation of monodomains is a uniform process already observed by Meyer *et al.* [14]. This paper addresses the dynamical aspects of the related systems of Finkelmann [13] and Mitchell [12], the statics of which is successfully described by the equilibrium theory [11,15,16]. Other more recent dynamical mechanical work by Clarke and Terentjev [20] shows that the apparent modulus varies significantly with frequency (in the range 0.2–20 Hz) if the imposed shears couple to the director, that is, where internal viscoelastic processes become involved.

ACKNOWLEDGMENTS

Financial support for P.I.C.T. from the Engineering and Physical Sciences Research Council (U.K.) is gratefully acknowledged. We are indebted to Dr E. M. Terentjev for discussions.

APPENDIX

The matrix of driving terms in the linearized equations of motion (16) is

$$M_{11}=2\Gamma_\theta\left\{-\left(1-\frac{1}{r}\right)[\lambda^2+(\overline{\delta^2}-\overline{\lambda_{xx}^2})r]\cos 2\overline{\theta}+2(r-1)\overline{\lambda}_{xx}\sin 2\overline{\theta}+A\lambda^2\cos 2\overline{\theta}\right\}, \tag{A1}$$

$$M_{12}=2\Gamma_\theta[-(r-1)\overline{\delta}\cos 2\overline{\theta}+\overline{\lambda}_{xx}(r-1)\sin 2\overline{\theta}], \tag{A2}$$

$$M_{13}=-2\Gamma_\theta[\overline{\lambda}_{xx}(r-1)\cos 2\overline{\theta}+\overline{\delta}(r-1)\sin 2\overline{\theta}], \tag{A3}$$

$$M_{21}=2\Gamma_\lambda[-(r-1)\overline{\delta}\cos 2\overline{\theta}+\overline{\lambda}_{xx}(r-1)\sin 2\overline{\theta}], \tag{A4}$$

$$M_{22}=2\Gamma_\lambda\left[1+\frac{3}{\lambda^2\overline{\lambda_{xx}^4}}+(r-1)\sin^2\overline{\theta}\right], \tag{A5}$$

$$M_{23}=-\Gamma_\lambda(r-1)\sin 2\overline{\theta}, \tag{A6}$$

$$M_{31}=-2\Gamma_\delta[\overline{\lambda}_{xx}(r-1)\cos 2\overline{\theta}+\overline{\delta}(r-1)\sin 2\overline{\theta}], \tag{A7}$$

$$M_{32}=-\Gamma_\delta(r-1)\sin 2\overline{\theta}, \tag{A8}$$

$$M_{33}=2\Gamma_\delta[r-(r-1)\sin^2\overline{\theta}]. \tag{A9}$$

Although not symmetric unless all Γ_α are equal, it must on physical grounds be a diagonalizable matrix with real eigenvalues.

In regime C, several elements of $\underline{\underline{M}}$ vanish, yielding

$$\underline{\underline{M}}_{\rm red}=\begin{pmatrix} 2\Gamma_\theta\left[\left(\frac{\lambda^2}{r}-\frac{1}{\lambda\sqrt{r}}\right)(r-1)-A\lambda^2\right] & \frac{2\Gamma_\theta(r-1)}{r^{1/4}\sqrt{r}} \\ \frac{2\Gamma_\delta(r-1)}{r^{1/4}\sqrt{r}} & 2\Gamma_\delta \end{pmatrix}, \tag{A10}$$

the eigenvalues of which are

$$\mu_{1,2}=(\lambda r)^{-1}[\Gamma_\delta\lambda r-\Gamma_\theta[(r-1)\sqrt{r}+\lambda^3(1-r+Ar)] \pm(4\Gamma_\theta\Gamma_\delta\lambda r[(r-1)r^{3/2}+\lambda^3(1-r+Ar)] +\{\Gamma_\delta\lambda r-\Gamma_\theta[(r-1)\sqrt{r}+\lambda^3(1-r+Ar)]\}^2)^{1/2}]. \tag{A11}$$

It is noteworthy that $\underline{\underline{M}}$ becomes singular for $\lambda=\lambda_1$ and $\lambda=\lambda_2$, and $\underline{\underline{M}}_{\rm red}$ for $\lambda=\overline{\lambda}_2$, i.e., at the boundaries between the different regimes. That is, at these points at least one eigenvalue vanishes and we have an intrinsically nonlinear problem, losing one of the exponentials to a power law. Then in the vicinity of λ_1 and λ_2 there is clearly a slowest mode and the remarks made in Sec. III about all variables either decaying together or one twice as fast as the other two are seen to apply.

[1] L. R. G. Treloar, *The Physics of Rubber Elasticity*, 3rd ed. (Clarendon Press, Oxford, 1975).
[2] R. T. Deam and S. F. Edwards, Philos. Trans. R. Soc. London, Ser. A **280**, 317 (1976).
[3] P. G. de Gennes, Phys. Lett. **28A**, 725 (1969).
[4] P. G. de Gennes, C. R. Seances Acad. Sci., Ser. B **281**, 101 (1975).
[5] G. G. Barclay and C. K. Ober, Prog. Polym. Sci. **18**, 899 (1993).
[6] L. Golubovic and T. C. Lubensky, Phys. Rev. Lett. **63**, 1082 (1989).
[7] J. Schätzle, W. Kaufhold, and H. Finkelmann, Makromol. Chem. **190**, 3269 (1989).
[8] G. R. Mitchell, M. Coulter, F. J. Davis, and W. Guo, J. Phys. II **2**, 1121 (1992).
[9] C. H. Legge, F. J. Davis, and G. R. Mitchell, J. Phys. II **1**, 1253 (1991).
[10] F. J. Davis and G. R. Mitchell, Polym. Commun. **28**, 8 (1987).
[11] P. Bladon, E. M. Terentjev, and M. Warner, J. Phys. II **4**, 75 (1994).
[12] G. R. Mitchell, F. J. Davis, and W. Guo, Phys. Rev. Lett. **71**, 2947 (1993).
[13] I. Kundler and H. Finkelmann, Makromol. Rapid Commun. **16**, 679 (1995).
[14] C.-C. Chang, L.-C. Chien, and R. B. Meyer, Phys. Rev. E **56**, 595 (1997).
[15] G. C. Verwey, M. Warner, and H. Terentjev, J. Phys. II **6**, 1273 (1996).
[16] H. Finkelmann, I. Kundler, E. M. Terentjev, and M. Warner, J. Phys. II **7**, 1059 (1997).
[17] E. M. Terentjev, M. Warner, R. B. Meyer, and J. Yamamoto (unpublished).
[18] M. Warner and E. M. Terentjev, Prog. Polym. Sci. **21**, 853 (1996).
[19] R. A. M. Hikmet and H. M. J. Boots, Phys. Rev. E **51**, 5824 (1995).
[20] S. M. Clarke and E. M. Terentjev (unpublished).
[21] P. G. de Gennes, in *Liquid Crystals of One- and Two-dimensional Order*, edited by W. Helfrich and G. Heppke (Springer, Berlin, 1980).
[22] P. D. Olmsted, J. Phys. II **4**, 2215 (1994).
[23] E. R. Zubarev, R. V. Talroze, T. I. Yuranova, N. A. Plate, and H. Finkelmann, Macromolecules **31**, 3566 (1998).
[24] P. I. C. Teixeira, Eur. Phys. J. B (to be published).
[25] R. Chasset and P. Thirion, in *Proceedings of the Conference on Physics of Non-Crystalline Solids*, edited by J. A. Prins (North-Holland, Amsterdam, 1965), pp. 345–359.
[26] S. M. Clarke and E. M. Terentjev, Phys. Rev. Lett. **81**, 4436 (1998).